16th World Conference on Earthquake, 16WCEE 2017

Santiago Chile, January 9th to 13th 2017

Paper N° 2062 (Abstract ID)

Registration Code: S-U1464684712

GROUND MOTION VARIABILITY FROM FINITE FAULT SIMULATIONS

F. Pacor(1), G. Ameri(2), F. Gallovic(3), M. D'Amico(4)

(1) *Researcher, INGV-Milano, francesca.pacor@ingv.it*
(2) *Seismologist, GEOTER – Fugro group, g.ameri@fugro.com*
(3) *Assistant Professor, Charles University, gallovic@karel.troja.mff.cuni.cz*
(1) *Researcher, INGV-Milano, maria.damico@ingv.it*

Abstract

The standard deviation (sigma) of the Ground Motion Prediction Equations (GMPEs) has a crucial impact on the results of seismic hazard analysis, especially for long return periods. Recently, great efforts have been made to find strategies to reduce sigma values, focusing on the different components that contribute to the ground-motion variability. This is an important task, since if the sources of ground motion variability are recognized, they could be accounted for the epistemic components of the uncertainties, thus reducing the aleatory component. To explore contributions related to site and propagations effects, specific dataset composed of records at the same site from different earthquakes or at multiple sites from events restricted in a given source-region can be used.

Strong-motion data can be hardly used to investigate the variability from a single fault, since different events on the same source have been recorded very rarely. To overcome this limitation, synthetic seismograms can represent a valid alternative to build a fault-specific dataset. In recent years, the use of numerical simulations is increasing and a number of initiatives worldwide promote their application for hazard assessment purposes.

When numerical simulations are used to predict future ground motions, a large number of possible earthquake scenarios on the same fault can be considered, varying the model parameters of the source-rupture process. Through the massive calculation of synthetic seismograms, the expected ground motion and associated variability at the site of interest can then be evaluated. However, to date, there is no standard approach to quantify and treat the generated ground-motion variability. In this paper, we explore the use of numerical simulations based on kinematic rupture models in order to treat the parametric variability of expected ground motions. Following the strategy adopted in the GMPE community, we generate synthetic dataset for single and multiple sites in the proximity of a single fault, considering numerous rupture scenarios. We establish a framework for treating the different components of the variability related to the synthetic datasets and quantify the contribution related to rupture scenarios and to the spatial distribution of sites with respect to the source. Since we use three simulation methods, we also evaluate how these components depend on the numerical approach.

Keywords: Finite-fault simulation, synthetic ground-motion variability, parametric aleatory variability

1. Introduction

The prediction of the ground motion amplitude generated by an earthquake at a given distance from the site of interest is a fundamental step for any seismic hazard assessment. This task is generally accomplished by adopting a set of empirical ground motion prediction equations (GMPEs). Beside the median predictions, the standard deviation (sigma, σ) has a crucial impact on the results of seismic hazard analysis [1] for long return periods.

In the last decade, great efforts have been made to find strategies to reduce sigma values associated to the GMPEs. A possible approach is to remove the ergodic assumption [2] according to which the variability at a single site from a specific source is the same as that derived from multiple site over large regions. In this direction, several studies [3, 4] showed that the sigma for an individual station is less than the overall sigma. A fundamental step toward the relaxation of the ergodic assumption is to identify and then correctly quantify the different components that contribute to the ground-motion variability. In fact, if the sources of ground motion variability are recognized, they could be accounted for as epistemic uncertainties, thus reducing the aleatory component.

The different components of ground motion variability are strictly related to the characteristic of the strong motion dataset adopted for the regression analysis [5]. Example are [6]: i) global datasets, including records at multiple sites from earthquakes occurred in different regions; ii) site-specific datasets, including multiple records at the same site from different earthquakes in different regions and iii) path-specific dataset, formed by records at the same site from earthquakes in a restricted source regions, than can be exploited to analyze specific propagation and site effects. One element that is missing in this list is the component of the ground motion variability related to a specific source that can be very important when the seismic hazard at a site is dominated by one particular fault (or fault segment). To analyze this kind of variability, strong motion data are limited, since different events on the same fault have very rarely been recorded. For example, [7] found only 8 pairs of repeated large earthquakes on the same source and showed that the between-event variability is reduced by about 45% and 80% with respect to global GMPEs.

Synthetic seismograms generated by kinematic or dynamic rupture models can represent a valid alternative to observed data, since they can be used to construct datasets with specific requirements by modelling many earthquake-site pairs in a given region [8]. These synthetic dataset has the advantage that any information on source, site and path are known, allowing to evaluate the different components of variability. Recently, some attempts in this direction have been carried out by [9, 10], that focused on the path and site terms in the South California and Marmara region, respectively.

In this study, we investigate the ground motion variability related to multiple ruptures on a single identified fault. The numerical simulations are used to generate a large number of possible rupture scenarios on the same fault, varying the model parameters of the source-rupture process [11, 12]. In this way, we obtain a synthetic dataset for single and multiple sites in the proximity of a single fault, considering a numerous of rupture episodes. We establish a framework for treating the different components of the variability related to these dataset and quantify the contribution related to rupture scenarios and to the spatial distribution of sites with respect to the source. Since we use three simulation methods, we also evaluate how these components depend on the numerical approach.

2. Method

The same formalism used in GMPEs is adopted for evaluating the components of the parametric variability in simulated ground-motions, as proposed in [13].

First, a dataset of synthetics at multiple sites from multiple rupture scenarios occurring on the same fault is computed. Then, a simple attenuation model with distance is calibrated on a synthetic dataset (one for each simulation method), in order to estimate the median ground motion from all scenarios at all the considered distances. The dispersion of synthetics with respect to the median ground motion represents the parametric aleatory variability.

Since each simulated rupture-scenario k contributes to the dataset with several synthetics for each virtual observer o, it is possible to separate the residuals R_{ko} into two contributions that we call between-scenario δB_k and within-scenario δW_{ko} residuals in the form:

$$R_{ko} = \delta B_k + \delta W_{ko} \tag{1}$$

Fig. 1 schematically illustrates the meaning of the terms δB_k and δW_{ko} in the synthetic ground motions, compared to the between-event and within-event residuals, as defined in the GMPEs.

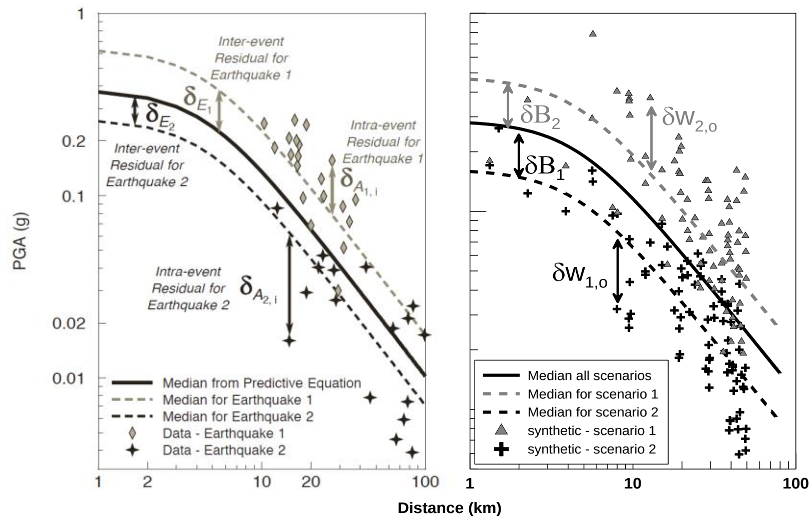

Fig. 1 – Left: Schematic illustration of between-event and within-event residuals for two earthquake of the same magnitude (from [14]). Right: schematic illustration of between-scenario (δB_k) and within-scenario (δW_{ko}) residuals for two rupture scenarios in the synthetic dataset considered in this study.

The *between-scenario terms* δB_k represents the average shift of the ground motion generated by a specific rupture scenario with respect to the median of all rupture scenarios. The *within-scenario terms* δW_{ko}, quantify the difference between the ground motion simulated at an individual observer o and the median ground motion relative to the specific rupture scenario k. The two residuals distributions are assumed independent and normally distributed, with between-scenario standard deviation σ_{BK} and within-scenario standard deviation σ_{WK}, respectively. The total standard deviation (σ) associated to median ground-motion simulated is $\sigma = \sqrt{\sigma_{BK}^2 + \sigma_{WK}^2}$

The *between-scenario standard deviation,* σ_{BK} is a measure of the ground motion variability among rupture scenarios, due to the variability in scenario-specific kinematic parameters (e.g., rupture velocity, slip distribution, etc.). The *within-scenario variability,* σ_{WK}, on the other hand, is a measure of the spatial ground-motion variability within each rupture scenario, depending on azimuthal variations of source-to-site configuration (e.g., directivity, radiation pattern, hanging/footwall effects).

Since each observer of the synthetic dataset is repeatedly sampled (multiple rupture scenarios are generated on the same grid of observers), the variability among observers can also be accounted for, following the same approach adopted in the empirical GMPEs (e.g. [15, 16]). In this case, the residuals are separated as:

$$R_{ko} = \delta B_o + \delta WO_{ko} \tag{2}$$

where the *between-observer term* δB_o quantifies the average shift of the ground motion simulated at specific observer *o* with respect to the median ground motion generated by all rupture scenarios. The *within-observer terms* δWO_{ko}, represent the difference of the ground motion generated by a single rupture scenario *k* and the median ground motion for specific observer *o*. Again, the two residuals distributions are assumed independent and normally distributed, with between-observer standard deviation σ_{BO} and within-observer standard deviation σ_{WO}, respectively. The total standard deviation σ associated to median ground-motion simulated is $\sigma = \sqrt{\sigma_{BO}^2 + \sigma_{WO}^2}$

The *between-observer standard deviation,* σ_{BO} is a measure of the ground motion variability among observers, due to site amplification or specific locations with respect to the source (e.g. radiation pattern, hanging/footwall effect). The *within-observer variability,* σ_{WO}, on the other hand, quantifies the ground-motion variability simulated at each observer, depending on azimuthal variations in source factors (e.g. directivity effects or proximity to the asperity).

3. Case study

Three synthetic datasets as compiled by [13] are used. The ground motion simulations are performed considering several rupture scenarios on the Irpinia fault (central Italy) that ruptured in 1980 producing a M 6.9 event. These datasets were constructed adopting different finite-fault simulation techniques: purely stochastic (EXSIM code, [17]), hybrid deterministic-stochastic with approximated Green's functions (DSM code, [18]), broadband hybrid integral-composite (HIC code, Gallovič and Brokešová, [19]) to generate synthetic ground motions at a dense grid of virtual receivers located around the fault up to distance of 50 km (Fig. 2).

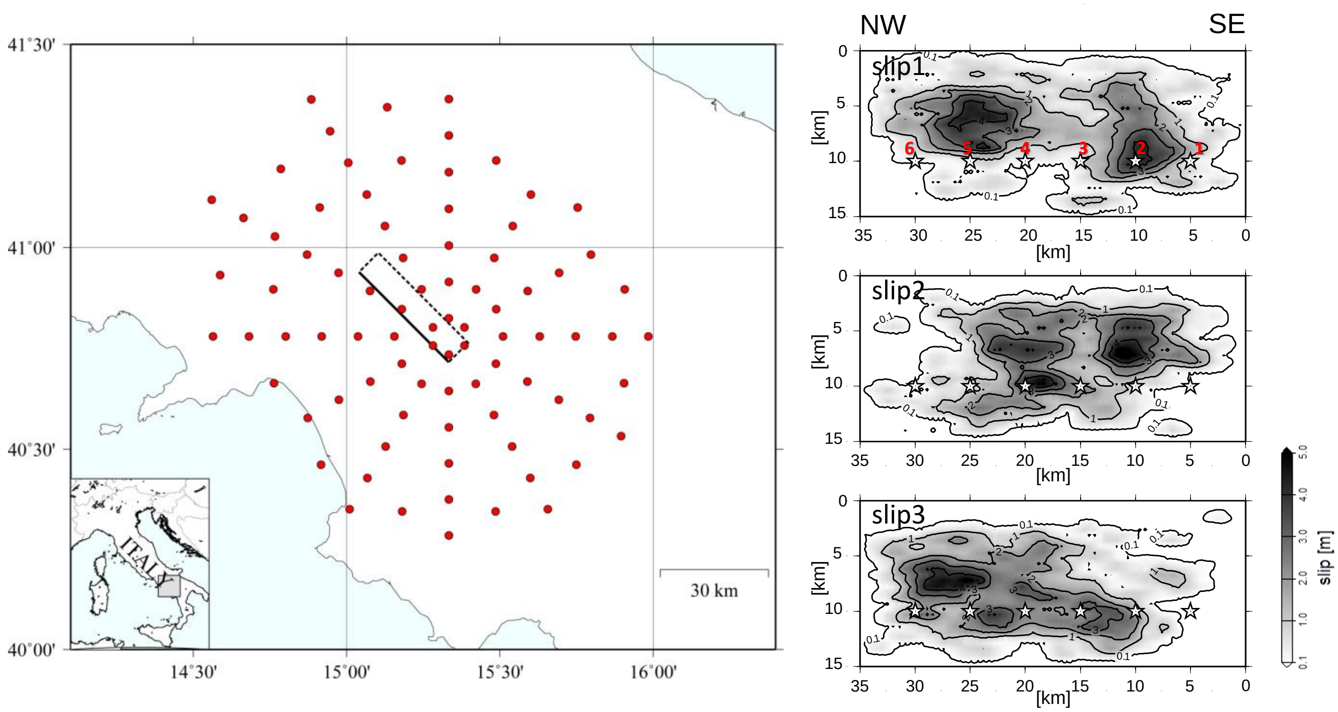

Fig. 2 – Left: Map view of Irpinia fault geometry and grid of virtual observers (red circles). Right: Slip models and nucleations points (from 1 to 6) adopted to generate different kinematic rupture models on the Irpinia fault.

For all simulations, a normal fault-plane, embedded in 1D propagation medium, 35 km long and 15 km wide, with 315° strike and 60° dip, was assumed. The magnitude was fixed to M=6.9 assuming the rupture of the entire fault segment that ruptured in 1980. On this fault, 54 different rupture models were simulated by varying the main source kinematic parameters such as: position of the nucleation point, rupture velocity, and final slip distribution (Fig. 2, see [13] for details). In this way, for each technique, the final dataset is composed of about 4500 synthetic seismograms. Since the modeling is performed adopting 1D propagation medium and bedrock sites, with no site amplification, these datasets can be exploited for investigating systematic effects related to the site-source configuration and source parameters.

3.1 Components of the total standard deviation

For each data set, the 5%-damped spectral accelerations are fitted using a simple model by applying a random effect approach (e.g., [20, 21]) that allows to separate the different components of the total residuals.

The model is:

$$Log_{10}(Y) = a + c_3\left(\sqrt{R_{JB}^2 + h^2}\right) \tag{3}$$

where Y is the spectral acceleration, R_{JB} is the Joyner-Boore distance (in Km) and *a*, *c* and *h* are coefficients to be determined in the regression. Note that magnitude is fixed as mentioned above. The regressions are performed twice: to evaluate i) the variability among the different rupture scenarios, and ii) among the different observers. Note that the total variance associated to the model is the same in both cases. Figure 3 shows the total standard deviation and its components, as a function of period T for the three simulation techniques. The total standard deviation depends on the technique and varies between 0.1 and 0.3 (in log10 units).

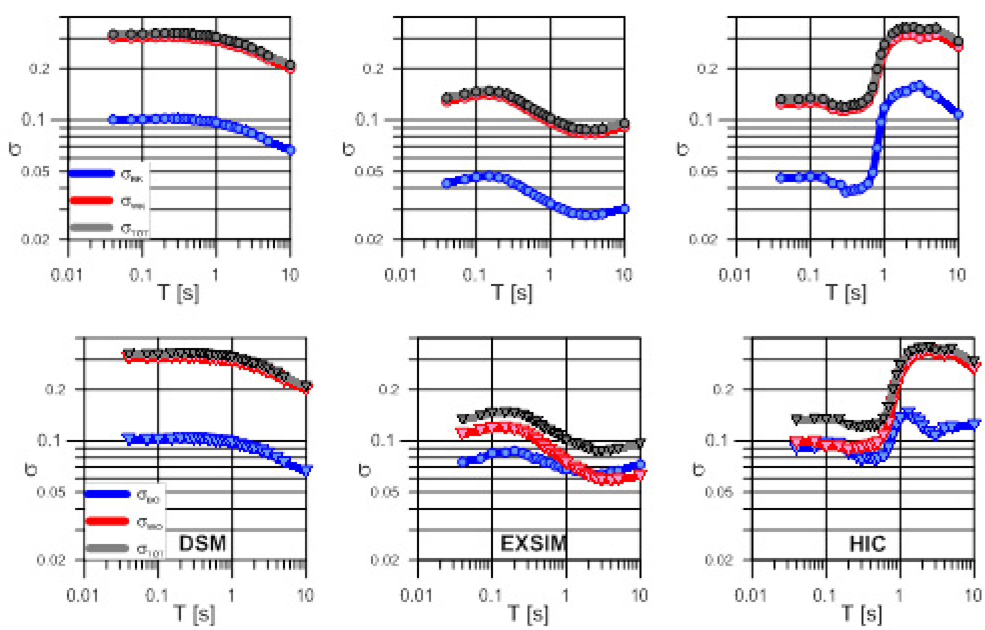

Fig. 3 – Top: Total (grey circle), between-scenario (blue circle) and within-scenario (red circle) standard deviations Bottom: Top: Total (grey triangle), between-observer (grey circle) and within-observer (red circle) standard deviations

The DSM and EXSIM ground motions have standard deviations quite constant with the period, assuming values around 0.3 and 0.15, respectively. For the HIC modelling, the variability abruptly changes around period T=1s, increasing from 0.12 to 0.32 at T = 10s. This variation occurs at the cross-over frequency, above which HIC simulates the radiated wave-field as an incoherent sum of point sources, similarly to the composite or purely stochastic approaches [22]. The within-scenario variability is the largest contribution to the total variability. This result suggests that the variability of the simulated ground motion, independently from the adopted code, is mainly controlled by effects that are related to the source-site position, such as directivity effect, that are described, in our analysis, by the within-residuals.

3.2 Between-scenario distribution of errors

The between-scenario residuals, defined in equation (1), are shown in Figure 4, considering the acceleration spectral ordinates SA at T=0.2 and T=2s. The source models are sorted by the rupture scenario ID. The analysis of the terms δB_K allows us to quantify the shift associated with each scenario of the dataset, with respect to median ground motion, given by Eq. 3.

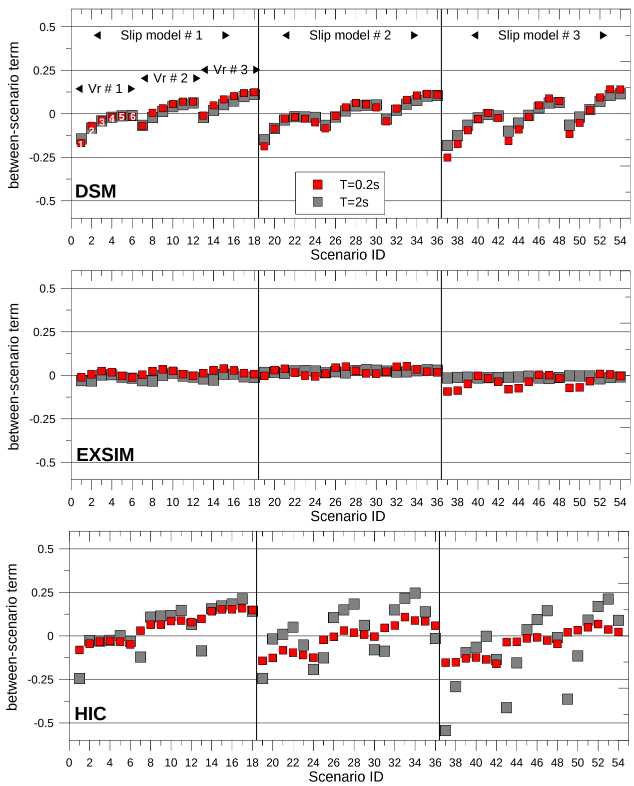

Fig. 4 – Top: Between-scenario residuals (or terms) at T=1s and T=0.2s for the three simulation codes. The top panel illustrate the corresponding rupture scenario parameters: rupture nucleation point (from 1 to 6), three rupture velocities, three slip models.

As an example, the DSM between-scenario residuals distribution show that scenario #1, characterized by slow rupture velocity, slip distribution with two asperities and rupture propagation toward Northwestern, has an residual of -0.15, which means that this scenario produce, on average, spectral ordinates that are a factor of 1.4 smaller than the median of all scenarios. In general, the between-scenario terms for DSM method are within the ±0.2 range and they have very similar trends both for long and short period.

For EXSIM method, the variability of the between-scenario residuals is small at all periods, with maximum absolute variations of a factor of 1.1. This result means that there is almost no influence of the variation of kinematic parameters in the average resulting ground motion, as also quantified by the very small σ_{BK} in Figure 3. Similarly, to EXSIM, at short periods HIC synthetics show moderate dependence on kinematic parameters, while they present the largest dispersion of between-scenario residuals at long periods. In this case, the scaling of the ground motion with rupture velocity is similar to what observed for DSM at all periods but there is a larger influence of the variation of slip distribution. Most of the residuals vary from -0.25 to 0.25, with some exceptions corresponding to the rupture models #37, #43 and #49, simulated with nucleation point #1, that predict much lower values than average at long period.

From the analysis of δB_K we can also infer some general considerations on the average effect of hypocenter position, average rupture velocity and slip distribution on the resulting ground motion. For instance, clearly evident is the scaling of the ground motion with increasing rupture velocity (for DSM and HIC), or the effect of a particular slip distribution (for HIC).

3.3 Between-observers distribution of residuals

In this case-study, the between-observer residuals quantify whether sites exhibit, on average, values larger or smaller than the mean, as a consequence of some effects related to the source-to-site configuration, regardless the particular rupture scenario (as the influence of each scenario has been averaged out).

In Figure 5a, the between-observer distributions are presented as a function of the Joyner-Boore distance R_{JB} (left panel) and of the source-to-site azimuth measured with respect to the center of the surface projection of the fault and clockwise from North.

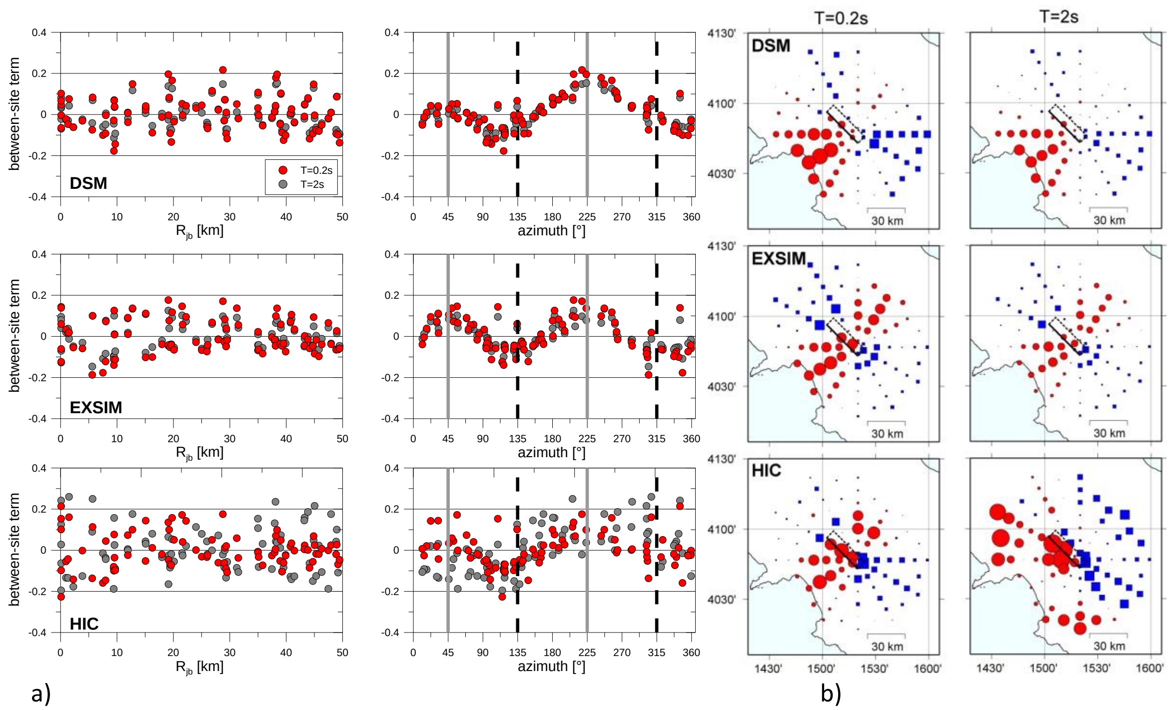

Fig. 5 - Between-observer (or between-site) residuals for the three simulation codes. a) Plotted versus distance and azimuth. The black-dashed and gray vertical lines represent the fault-strike direction (strike of the fault is 315°) and the fault-dip direction (i.e. up-dip direction is 225°, the perpendicular to the fault strike), respectively. b) Map distributions. Red and blue circles indicate positive and negative values, respectively. The symbol dimension is proportional to the absolute value of the residuals.

The between-observer residuals do not show any particular trend with distance both at short and long periods, which means that the attenuation of the median curve correctly describes the general attenuation of the simulated motion from the source. On the contrary, the residuals plotted versus azimuth show a trend, that is related with the fault strike and dip directions. Although the distribution depends on the simulations methods, the largest positive values occur for sites located along dip direction.

To better understand these patterns, Figure 5b illustrates the spatial distribution of between-observers residuals. For DSM and the long period component of HIC, the sites located in the up-dip direction (about 225°) present a ground motion systematically larger than the median motion, since the considered hypocenters (see Fig. 2) are all located at 10 km along the dip of the fault (i.e., in the lower half of the fault), thus producing an up-dip directivity effect that is present in all rupture scenarios. The azimuthal distribution of HIC residuals is more complex than the DSM one, since the up-dip rupture propagation and radiation pattern (that in our case-study is fixed) affect the ground motion in a combined way.

For EXSIM and for the high-frequency components of HIC, the positive residuals in the fault-dip direction are very similar. Both the composite and the stochastic models compute the ground motion by an incoherent sum of the motions from point-sources located on the extend source. As shown by [23], when the point-sources are randomly distributed, the resulting ground motion at a given site scales with an "effective distance", R_{EFF}, that accounts for geometrical spreading from various parts of a finite fault. R_{EFF} assumes smaller values for sites located perpendicularly to the midpoint of the fault compared to observers off the tip of the fault, thus causing larger motions.

3.4 – Synthetic-to-synthetic residuals distribution

The synthetic-to-synthetic residuals (δWS_{ko}) represent the remaining residuals after that the average contributions of the scenarios (δB_K) and the observers (δB_o) have been removed:

$$\delta WS_{k,o} = R_{ko} - \delta B_k - \delta B_o \tag{4}$$

This term depends on both rupture scenario and observer location. Effects such as the along-strike directivity, that changes as a function of the reciprocal position between nucleation points and observers are included in this component. The synthetic-to-synthetic variability represent the largest contribution to the total variability for DSM and for HIC at long periods with values within +/-0.8 (Figure 6). The EXSIM and HIC short period these residuals are much lower, not exceeding 0.2 in absolute value.

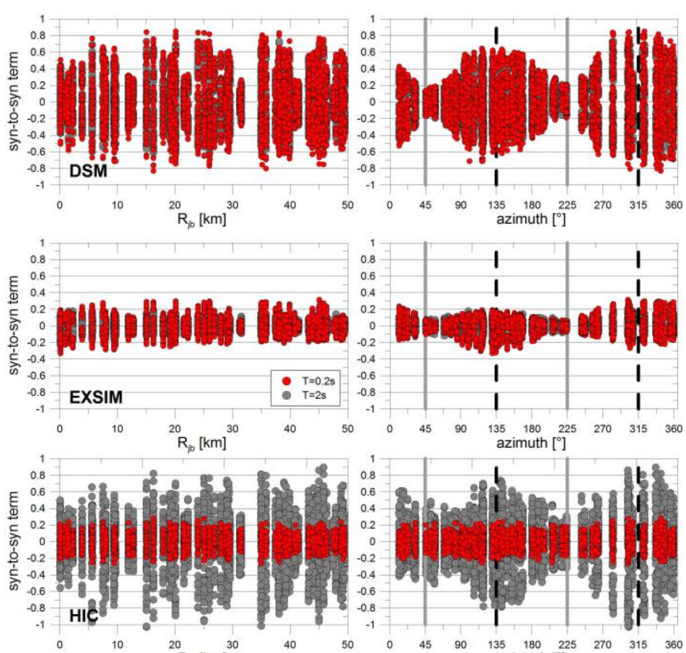

Fig. 6 – Synthetic-to-synthetic residuals for the three simulation codes plotted versus Joyner-Boore distance (left) and azimuth (right). The black-dashed and gray vertical lines represent the fault-strike direction (strike of the fault is 315°) and the fault-dip direction (i.e. up-dip direction is 225°, the perpendicular to the fault strike), respectively.

Fig. 6 shows the synthetic-to-synthetic residuals as a function of distance and azimuth. While no dependence on distance is observed, a clear trend can be recognized with respect to the azimuth, with larger dispersion occurring in the strike-parallel direction (black dashed lines in Figure 6). This is due to the presence of different scenarios producing forward and backward directivity at the same observer (opposite location of the nucleation point on the fault). On the contrary, smaller variability is found in the strike-normal directions (gray lines). This feature is clearly visible for DSM, both at short and long periods, and for HIC, but only for long periods. The EXSIM simulations show a weaker azimuthal dependence, but with the same characteristics of the other two simulation codes.

4. Discussion and conclusion

In case of probabilistic seismic hazard assessment for sites where the hazard is controlled by a single local fault, it is important to relax the ergodic assumption also in terms of source variability and not only in terms of site and path.

We evaluated the various components of parametric variability of ground motions simulated by considering several ruptures scenarios on a single fault, using the same approach largely adopted in GMPEs. From synthetic data sets, generated with different simulation techniques, we estimated the different terms of variability: i) the total variability, σ_{TOT}; ii) the between-scenario variability, σ_{BK}; iii) the between-observer variability, σ_{BO}; v) the remaining variability (that we called synthetic-to-synthetic variability σ_{SY}).

The analyses performed considering a single fault on which several ruptures can occur, suggest the following outcomes:

- the total standard deviation σ_{TOT} depends on the adopted simulation method, although the same variations of the input parameters are considered and source-to-site geometry is fixed. EXSIM, which represents the simplest simulation approach to predict ground motion, provides the lowest σ_{TOT}.
- The largest contribution to the total sigma is given by the synthetic-to-synthetic component (σ_{SY}) for all techniques (particularly evident in EXSIM simulations), meaning that the fault rupture processes are the main source of the spatial variability. This is not surprising because the no local site effect or 3D path effect is included in our simulations.
- The between-observer sigma, σ_{BO}, accounts for variability due to the fixed source-site configuration. It contributes to the total spatial variability of simulated motions due, for example, to the radiation pattern of the source that produce ground motion systematically higher or lower than the median at particular sites. It is found to be of the same order or smaller than the between-scenario variability
- At long period, HIC has the largest between-scenario standard deviation, σ_{BK}. This means that the ground motion generated by more sophisticated simulation techniques (e.g., including complete wavefield and correctly accounting for long-wavelength contributions of the seismic source), as expected, is more sensitive to variations in source kinematic parameters than the stochastic methods.
- This study provides insights on the variability of the ground motion related to rupture scenarios on a single fault source. This is particularly useful because ground motions records from multiple rupture episodes on the same fault are lacking. In modern PSHA software (e.g., OpenQuake, Crisis, Frisk88) the fault plane is sampled with ruptures of different sizes and variable hypocenter positions in order to include uncertainties in rupture location in the hazard integral. However, the aleatory variability of the ground motion estimates for such cases may not be adequately represented by the sigma of the GMPEs because the between-event variability of GMPEs generally represents the variability among earthquakes on different faults. Fig. 7 shows the comparison of the empirical between-event variabilities and the between-scenario variabilities (σ_{BK}) estimated in this case-study. Our results confirm that, in case of a seismic hazard assessment controlled by a single fault, the between-event variability could be reduced, as suggested by [7] and that the extension of this reduction could be quantified by means of finite-fault simulations.

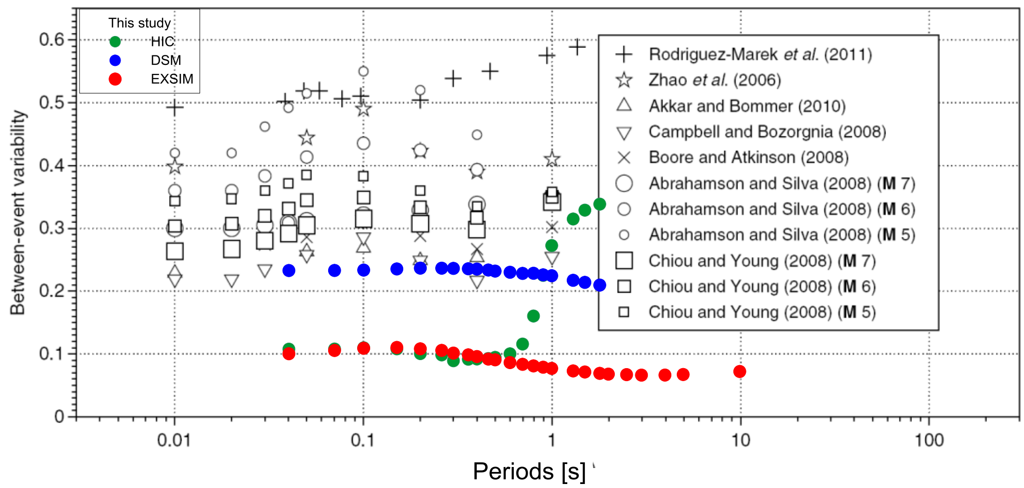

Fig. 7 – Between-event variability of recent ground-motion predictive equations compared with the between-scenario variability estimated in this study for the Irpinia fault (modified by [24]).

5. References

[1] Bommer JJ, Abrahamson NA (2006): Why do modern probabilistic seismic-hazard analyses often lead to increased hazard estimates? *Bulletin of the Seismological Society of America*, **96** (6), 1967–1977.

[2] Anderson JG, and Brune JN (1999): Probabilistic Seismic Hazard Analysis without the Ergodic Assumption, *Seismological Research Letter*, **70** (1), 19–28

[3] Atkinson GM (2006): Single-Station Sigma, *Bulletin of the Seismological Society of America*, **96** (2), 446–455, doi:10.1785/0120050137

[4] Rodriguez-Marek A, Montalva GA, Cotton F, Bonilla F (2011): Analysis of Single-Station Standard Deviation Using the KiK-net Data, *Bulletin of the Seismological Society of America*, **101** (3), 1242–1258, doi:10.1785/0120100252

[5] Walling MA (2009): Non-ergodic probabilistic seismic hazard analysis and spatial simulation of variation in ground motion. *PhD dissertation*., University of California, Berkeley

[6] Atik L, Abrahamson NA, Bommer JJ, Scherbaum F, Cotton F, Kuehn N (2010): The Variability of Ground-Motion Prediction Models and Its Components, *Seismological Research Letter*, **81** (5), 794–801, doi:10.1785/gssrl.81.5.794

[7] Yagoda-Biran G, Anderson JG, Miyake H, Koketsu K (2015): Between-Event Variance for Large Repeating Earthquakes, *Bulletin of the Seismological Society of America*, 105, 2023-2040, doi:10.1785/0120140196.

[8] Graves R, Jordan TH, Callaghan S, Deelman E, Field E, Juve G, Kesselman C, Maechling P, Mehta G, Milner K, Okaya D, Small P, Vahi K(2010): CyberShake: A Physics-Based Seismic Hazard Model for Southern California, *Pure Applied Geophysics*, **168**, 367-381, doi:10.1007/s00024-010-0161-6.

[9] Villani M, Abrahamson NA (2015): Repeatable Site and Path Effects on the Ground-Motion Sigma Based on Empirical Data from Southern California and Simulated Waveforms from the CyberShake Platform, *Bulletin of the Seismological Society of America*, **105**, 2681-2695, doi:10.1785/0120140359.

[10] Douglas J, Aochi H (2016): Assessing Components of Ground-Motion Variability from Simulations for the Marmara Sea Region (Turkey), *Bulletin of the Seismological Society of America*, **106** (1), 300-306.

[11] Cultrera G, Cirella A, Spagnuolo E, Herrero A, Tinti E, Pacor F (2010): Variability of Kinematic Source Parameters and Its Implication on the Choice of the Design Scenario, *Bulletin of the Seismological Society of America*, **100**, 941-953, doi:10.1785/0120090044.

[12] Ameri G, Gallovic F, Pacor F, Emolo A (2009): Uncertainties in Strong Ground-Motion Prediction with Finite-Fault Synthetic Seismograms: An Application to the 1984 M 5.7 Gubbio, Central Italy, Earthquake, *Bulletin of the Seismological Society of America*, **99**, 647-663, doi:10.1785/0120080240.

[13] Ameri G, Emolo A, Pacor F, Gallovic F (2011): Ground-Motion Simulations for the 1980 M 6.9 Irpinia Earthquake (Southern Italy) and Scenario Events, *Bulletin of the Seismological Society of America*, **101**, 1136-1151, doi:10.1785/0120100231.

[14] Strasser FO, Abrahamson NA, Bommer JJ (2009): Sigma: Issues, Insights, and Challenges, *Seismological Research Letter*, **80** (1), 40–56, doi:10.1785/gssrl.80.1.40

[15] Bindi D, Luzi L, Pacor F (2009): Interevent and interstation variability computed for the Italian accelerometric archive (ITACA). *Bulletin of the Seismological Society of America*, **99** (4): 2471–2488. doi:10.1785/0120080209

[16] Bindi D, Luzi L, Pacor F, Paolucci R (2011): Identification of accelerometric stations in ITACA with distinctive features in their seismic response, *Bulletin of Earthquake Engineering*, **9** (6), 1921–1939. doi:10.1007/s10518-011-9271-5

[17] Motazedian D, Atkinson GM (2005): Stochastic finite-fault modeling based on a dynamic corner frequency. *Bulletin of the Seismological Society of America*, **95**, 995–1010.

[18] Pacor F, Cultrera G, Mendez A, Cocco M (2005): Finite Fault Modeling of Strong Ground Motions Using a Hybrid Deterministic-Stochastic Approach, *Bulletin of the Seismological Society of America*, 95, 225-240, doi:10.1785/0120030163.

[19] Gallovič F, Brokešová J (2007): Hybrid k-squared source model for strong ground motion simulations: Introduction, *Physics Earth Planet Interior*, **160**, 34–50.

[20] Brillinger DR, Preisler HK (1985): Further analysis of the Joyner-Boore attenuation data, *Bulletin of the Seismological Society of America*, **75** (2), 611–61422

[21] Abrahamson NA, Youngs RR (1992): A stable algorithm for regression Analyses using The Random Effects Model *Bulletin of the Seismological Society of America*, **82** (1), 505–510

[22] Gallovič F, Burjánek J (2007): High-frequency Directivity in Strong Ground Motion Modeling Methods, *Annals of Geophysics*, **50** (2), 203-211.

[23] Boore D. (2009): Comparing Stochastic Point-Source and Finite-Source Ground-Motion Simulations: SMSIM and EXSIM, *Bulletin of the Seismological Society of America*, **99** (6), 3202-3216, 10.1785/0120090056.

[24] Cotton F, Archuleta R, Causse M (2013): What is Sigma of the Stress Drop*? Seismological Research Letters*, **84** (1), 42-48.